Recent Results from MRX: Magnetic Reconnection Experiments in a Controlled Laboratory Setting

Masaaki Yamada, Hantao Ji, and Scott Hsu
Princeton Plasma Physics Laboratory, Princeton, NJ 08543 USA

The Magnetic Reconnection Experiment (MRX) is the most recent experiment dedicated to investigate the fundamental physics of magnetic reconnection. The primary objective of MRX is the fundamental study of reconnection using a very flexible merging toroidal plasma configuration. The overall plasma geometry is axisymmetric (hence 2-D) but can be made non-axisymmetric to study 3-D characteristics of merging. These plasmas have a high conductivity, which is characterized by a measured Lundquist number $S > 10^3$, and ion gyro-radii much smaller than the plasma size.

The goal of the initial work has been to create a number of different initial states and to address the following issues: (1) Can one create the familiar axisymmetric 2-D reconnection layer? Does the reconnection process remain axisymmetric or will 3-D phenomena spontaneously occur? (2) How does the reconnection rate depend on the third component of the merging field? (3) What is the dependence of the reconnection rate on global MHD forces, which can be controlled by external boundary conditions? (4) And how are MHD plasma flows associated with reconnection generated and converted to heat? The first two issues above have been addressed in recent papers [Yamada et al. 1997 (1) & (2); Ji et al., 1998]. In all these areas, it is believed that the interrelationship between the global magnetic configuration and the resistive reconnection region will play a key role in determining the reconnection features.

MRX Experimental Setup

The MRX device creates an environment to satisfy the criteria for MHD plasma ($S \gg 1$, $\rho_i \ll L$) and the boundary condition can be controlled externally. Two flux cores with 37.5 cm major radii and 9.5 cm minor radii are installed in the vacuum vessel. Inside each core, there is a 4-turn coil that carries a toroidal current and a helical 36-turn toroidal solenoid. By properly programming currents in the toroidal coils and solenoids, plasma current and toroidal field can be prescribed independent of the sense of helicity in the toroidal solenoid. The MRX device generates two annular plasmas by inducing currents around the two flux cores. Initial MRX experiments have been carried out in the double annular plasma set-up in which two toroidal plasmas with annular cross section are formed independently around two flux cores and magnetic reconnection is driven in the quadrupole field, as shown in Fig. 1(a). Each flux core (darkened section in Fig. 1(a)) contains a toroidal field (TF) coil and a poloidal field (PF) coil. By pulsing currents in the TF coils after a quadrupole poloidal magnetic field is established by the PF coil currents, plasmas are created around each flux core by induction [Yamada et al., 1997].

Initial Experimental Results

After the annular plasmas are created, the PF coil current can be increased or decreased. In the case of increasing PF current (Fig. 1(b)), the poloidal flux in each plasma is "pushed" toward the X-point (push mode). In the case of decreasing PF current (Fig. 1(c)), the poloidal flux in the common plasma is "pulled" back toward the X-point (pull mode).

In the initial MRX experiments the "pull" mode has been studied intensively with and without the third vector component (toroidal or azimuthal direction) of the magnetic field. To document the internal magnetic structure of the reconnection in a single shot, a 2-D magnetic probe array is placed in an R-Z plane as shown in Fig. 2(a). Plasma parameters are: $B \sim 0.5\text{-}1.0$ kG, $T_e \sim 10\text{-}30$ eV, and $n_e \sim 0.1\text{-}1.0 \times 10^{14}$ cm^{-3}.

Two distinctively different shapes of neutral sheet current layers are identified; the shape depends on the third vector component of the reconnecting magnetic field. Fig. 2(b) & (c) show the time evolution of the poloidal flux contours during reconnection of co-helicity (with toroidal field) and null-helicity (without toroidal field) plasmas. The contours are derived, assuming axisymmetry (assured by a center conductor placed along the major axis), from the 2-D magnetic probe array measurements. Other operational conditions are held constant for each discharge. When no magnetic reconnection is induced, a typical X-shape separatrix region is observed as seen at t=260 μs in both Fig. 2(b) & (c). As poloidal flux is driven toward the diffusion region, a neutral sheet forms. Without the third component, a thin double-Y shaped diffusion region is clearly identified (Fig. 2(c)). With a si\zable third component, an O-shaped sheet current appears (Fig. 2(b)). This O-point current channel grows into a spheromak configuration. To our knowledge, this is the clearest experimental distinction between current sheets whose shapes depend on the

third component of the merging field. The neutral current sheet for the null-helicity case is much narrower than for the co-helicity case. It is found that merging of null-helicity plasmas occurs much faster than merging of co-helicity plasmas.

The current density evaluated by magnetic probe data provides the profile of the neutral sheet current for the same sequence of shots. A near symmetric profile of neutral sheet current was observed for null-helicity reconnection, and the width is always much narrower than that of the co-helicity case.

To accurately measure the width of the neutral sheet, a very fine scale internal probe array, in which micro-scale magnetic probes are linearly placed with 5 mm spacing, is inserted into the MRX plasma. The time evolution of B_Z gives the radial profile evolution of the neutral sheet current based on the relationship $j_t = dB_Z/dR$ ($dB_R/dz=0$ for null-helicity) at the center of the machine, Z=0. For co-helicity merging, the transition of the merging angle is gradual and smooth. But for null-helicity merging, the pitch of the field lines changes abruptly at the reconnection point. One observes a steepening of the magnetic field profile at the diffusion region along with a sharpening of the neutral sheet current.

It is also important to note that the data points for null-helicity merging fit very well, if not exclusively, into $B_Z=\arctan[(R-R_0)/R_0]+ b(R-R_0)$, thus leading to $j_t = 1/[(R-R_0)^2+d^2]+C$. This excellent fit leads to accurate evaluation of the thickness of the neutral sheet, which is seen to be as narrow as 1 cm, which is of the order of the ion gyro-radius ρ_i. It decreases as the magnetic field is raised, which appears to be due to the dependence of ρ_i on B or to the increased density [Yamada et al., 1997(2)].

Experimental Test of the Sweet-Parker Model on MRX

Although the Sweet-Parker model [Sweet, 1958; Parker, 1957] was proposed forty years ago, its validity has been questioned because its predicted reconnection rate is too slow to explain explosive solar flares. Instead, the attention has shifted to Petschek's model [Petschek, 1964] which predicted faster reconnection rates. Despite numerous theoretical and computational work published on these models, none of the models have been verified or tested rigorously in the laboratory or in space.

In MRX, a comprehensive test of the Sweet-Parker model has been carried out [Ji et al., 1998)]. All basic parameters are measured including magnetic field profile, electron density, electron temperature, and reconnection speed V_R. In Fig. 3 (a), the reconnection rate (V_R/V_A) is plotted against $1/\sqrt{S}$ where the Lundquist number is calculated from the Spitzer resistivity. Obviously, the classical Sweet-Parker model cannot explain the observed reconnection rate. However, causes of the discrepancy were found by systematically examining the validity of Ohm's law, the continuity equation, and the momentum equation. Examination of the Ohm's law revealed that the measured resistivity was greatly enhanced over its classical value in the collisionless regime (see the last section). However, the observed reconnection rate could be explained if the effective resistivity was used to calculate S. Also it was found that both finite compressibility and downstream pressure had a significant effect on the reconnection rate. A generalized Sweet-Parker model was formulated to incorporate compressibility and downstream pressure and to employ the effective resistivity [Ji et al.1998]. The reconnection rate is then given as $V_R/V_A= (1/\sqrt{S^*})\sqrt{[(V_Z+(L/n)\partial n/\partial t)/V_A]} \equiv 1/\sqrt{S_{eff}}$. Here S^* is the Lundquist number calculated from the effective resistivity. Figure 3(b) shows good agreement between the observed reconnection rate and the prediction from the generalized model, $V_R/V_A = 1/\sqrt{S_{eff}}$.

Summary and Discussions

In summary we have reviewed recent results from MRX magnetic reconnection experiments in a controlled laboratory setting. Extensive data have been obtained in MHD plasmas of S=100-1000.

One of the most important achievements is the experimental verification of a generalized Sweet-Parker model [Ji et al., 1998]. In this recent work it is found that the observed reconnection rate can be explained by a generalized Sweet-Parker model which incooperates compressibility, downstream pressure, and the effective resistivity. The latter is often significantly enhanced over its classical values in the collisionless limit. A significant implication of this result is that the Sweet-Parker model with generalizations is valid in certain 2-D reconnection cases with axisymmetric geometry. A question might be raised: can Petschek-type models explain the same observations? Direct comparisons, however, are not possible since these shock-based models do not give definite predictions on reconnection rates but only their maxima. It is possible that the Lundquist number and/or the driving electric field in MRX plasmas are too small to produce such a shock structure. Extended operation to higher S and more strongly driven reconnection is planned in MRX to investigate the validity of Petschek-type models.

An important question regarding the current sheet is its thickness, which is an important indicator of the nature of reconnection. In MHD plasmas, the thickness of this thin current layer is found to be on

the order of the ion gyro-radius and decreases as magnetic field is raised [Yamada et al., 1997(2)]. Both in the geomagnetic tail region and the magnetopause, it has been often observed that the thickness is also on the order of the ion gyro-radius [Kivelson and Russell, 1995]. The precise thickness has been successfully measured in MRX by a very fine-scale magnetic probe array. It is indeed found that the thickness is proportional to the ion gyro-radius as well as the ion skin depth. In the null-helicity case, the ion gyro-radius is on the order of the ion skin depth. Since $B^2/2\mu_0 = nkT_i$ leads to $c/\omega_{pi} = \rho_i$, this indicates that the magnetic pressure in the upstream region is balancing the plasma kinetic pressure in the reconnection region.

Another important finding to date is that the enhancement factor of the measured resistivity over its classical values (or "the anomaly factor") is strongly dependent on collisionality. The experimental values of the electrical resistivity are obtained by dividing electric field by the measured current density. The electric field is calculated by taking the time derivative of the poloidal flux from the magnetic probe measurements. In the collisional regime where the mean-free-path is comparable to the current sheet thickness, the anomaly factor is near unity, i.e. almost no resistivity enhancement is found. However, in the collisionless regime where the mean-free-path is much longer than current sheet thickness, the anomaly factor is increased to about 10 in both TS-3 [Ono et al., 1993] and MRX and a factor of more than 100 in LPD [Gekelman et al., 1982], a significant enhancement over the classical value. Although this is most likely due to wave-particle interactions, a definitive study is needed to find a relationship between the observed enhanced resisitivity and the amplitude of specific waves. This will be the subject of intensive investigation in MRX experiments in the future. We note that the accessibility of collisionless reconnection has great relevance to magnetospheric phenomena, which almost always occur in the collisionless regime.

References

Gekelman, W. et al., "Magnetic Field Line Reconnection Experiments: 3," J. Geophys. Res. **87**, 101 (1982).

Ji, H., M. Yamada, S. Hsu, and R. Kulsrud, "Experimental test of the Sweet-Parker model of Magnetic Reconnection," Phys. Rev. Letts. **80**, 3256 (1998).

Kivelson G. and C.T. Russell, *Introduction to Space Physics* (Cambridge University Press, London, 1995).

Ono, Y. et al., "Experimental Investigation of Three-dimensional Magnetic Reconnection by use of Two Colliding Spheromaks," Phys. Fluids B **5**, 3691 (1993).

Parker, E.N., "Sweet's Mechanism for Merging Magnetic Fields in Conducting Fluids," J. Geophys. Res. **62**, 509 (1957).

Petschek, H.E., "Magnetic Field Annihilation," NASA Spec. Pub. SP-50, 425 (1964).

Sweet, P. A., "The neutral point theory of solar flares," *in Electromagnetic Phenomena in Cosmical Plasmas* (Cambridge University Press, New York, 1958).

Yamada, M. H. Ji, , S. Hsu, T. Carter, R. Kulsrud, N. Bretz, F. Jobes, Y. Ono, and F. Perkins, "Study of Driven Magnetic Reconnection in a Laboratory Plasma," Phys. Plasmas **4**, 1936 (1997).

Yamada, M., H. Ji, S. Hsu, T. Carter, R. Kulsrud, Y. Ono, and F. Perkins, "Identification of Y-shaped and O-shaped Diffusion Regions during Magnetic Reconnection in a Laboratory Plasma," Phys. Rev. Letts. **78**, 3117 (1997).

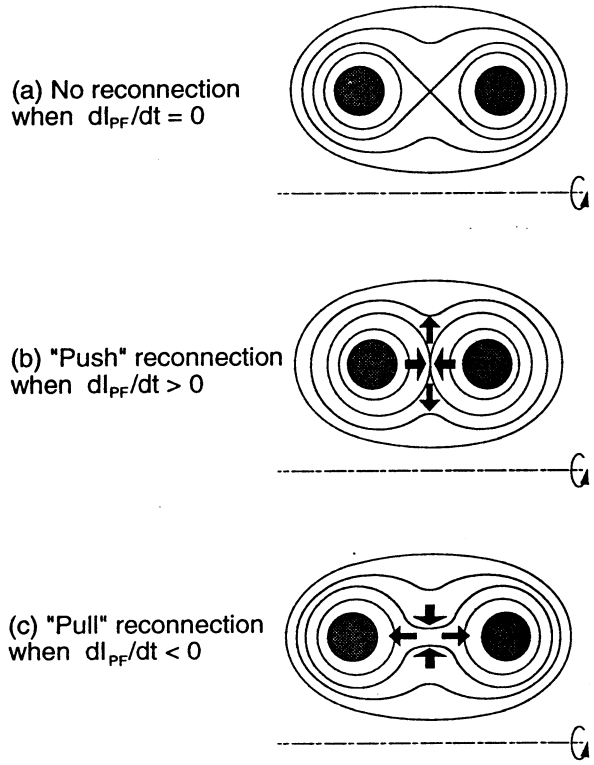

Fig. 1. Magnetic configuration during (a) no reconnection (b) push mode, and (c) pull mode.

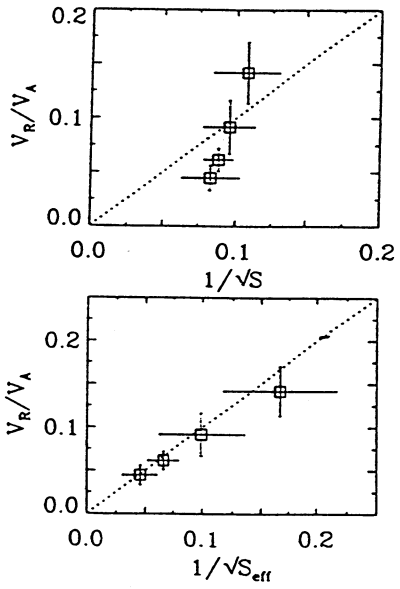

Fig. 3. Comparison of measured reconnection rate with (a) classical Sweet-Parker model and (b) new generalized mod

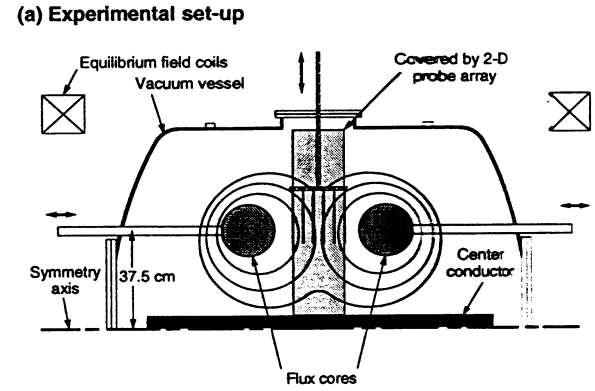

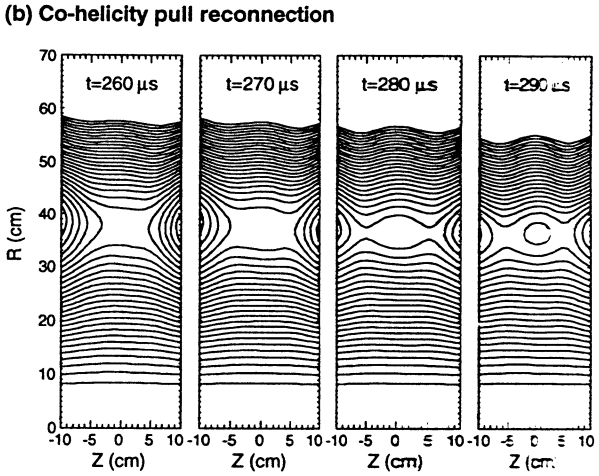

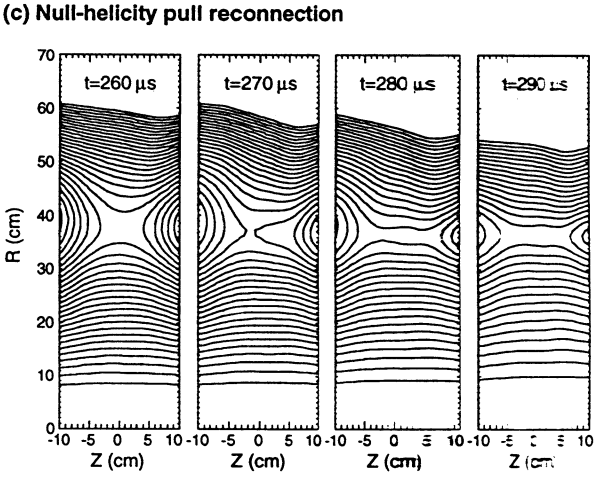

Fig. 2. (a) Experimental setup including 2-D magnetic probe array. Poloidal flux contour time evolution for (b) co-helicity and (c) null-helicity reconnection.